Malaysian Journal of Analytical Sciences (MJAS)
Published by Malaysian Analytical Sciences Society

NECROSIS AND LATE APOPTOSIS OF SILVER NANOPARTICLES PRODUCED USING MARINE BACTERIUM-DERIVED RHAMNOLIPID AGAINST HepG2 AND MCF-7 CELLS

(Nekrosis aan Apoptosis Lewat Nanopartikel Perak yang dihasilkan Menggunakan Ramnolipid dari Bakterium Laut Terhadap Sel HepG2 Dan MCF-7)

Lara Al-Smadi[1], Ghaith H Mansour[2], Tan Suet May Amelia[1,3], Noor Aniza Harun[1], and Kesaven Bhubalan[1,4]*

[1]*Faculty of Science and Marine Environment, Universiti Malaysia Terengganu, 21030 Kuala Nerus, Terengganu, Malaysia*
[2]*Department of Allied Medical Sciences, Zarqa University College, Al-Balqa Applied University, Jordan*
[3]*Department of Biomedical Sciences, Chang Gung University, Guishan, Taoyuan, 333, Taiwan*
[4]*Institute of Climate Adaptation and Marine Biotechnology (ICAMB), Universiti Malaysia Terengganu, 21030 Kuala Nerus, Terengganu, Malaysia*

**Corresponding author: kesaven@umt.edu.my*

Received: 20 June 2024; Accepted: 7 October 2024; Published: 29 December 2024

Abstract

Liver and breast cancers are severe illnesses since they directly impact vital organs of the body. Recently, nanomedicine has emerged as a prominent option for the treatment of these lethal diseases. Consequently, several nanoparticles have been used to target cancer cell lines. Silver nanoparticles (AgNPs) have the greatest degree of biocompatibility among other types of nanoparticles. This study aims to examine the cytotoxicity, apoptosis, and necrosis effects of AgNPs that were synthesised utilising marine bacterium-derived rhamnolipid (RL-AgNPs) from *Pseudomonas aeruginosa* UMTKB-5 against HepG2 and MCF-7 cells. Cytotoxicity assays were conducted to evaluate substance toxicity. Furthermore, the induction of apoptosis and the dispersion of cell cycles were examined using flow cytometry. After 48 hours of treatment, findings showed that the half-maximal inhibitory concentration (IC_{50}) value for RL-AgNPs was 67.42 µg/mL in HepG2 cells and 7.4 µg/mL in MCF-7 cells. Flow cytometry analysis showed a significant rise in apoptotic and necrotic cells in the group treated with RL-AgNPs, compared to the control group, in both cell lines. Moreover, there were modifications in the proportion of cells retained in different stages of the cell cycle, relative to the control group. In addition, it was shown that RL-AgNPs (IC_{50}) triggered apoptosis in HepG2 and MCF-7 cells, as evidenced by the accumulation of the sub-G1 phase. Overall, RL-AgNPs have the potential to serve as an anticancer agent due to their capacity to trigger apoptosis in cancer cells, hence promoting cell cycle exit and possibly aiding in the development of future therapeutic drugs for cancer therapy.

Keywords: Silver nanoparticles, rhamnolipid, HepG2, MCF-7, cytotoxicity

Abstrak

Kanser hati dan payudara merupakan penyakit yang kritikal kerana memberi kesan secara langsung kepada organ penting badan. Baru-baru ini, perubatan nano telah dianggap sebagai alternatif unggul untuk rawatan penyakit maut ini. Justeru itu, keluaran sel kanser telah dirawat dengan pelbagai nanopartikel. Nanopartikel perak (AgNPs) adalah yang paling biokompatibel daripada beberapa jenis zarah nano. Kajian ini bertujuan untuk menyiasat kesan nekrosis, apoptosis dan sitotoksisiti nanopartikel perak yang

disintesis menggunakan ramnolipid bacterium laut (RL-AgNPs) daripada *Pseudomonas aeruginosa* UMTKB-5 terhadap sel HepG2 dan MCF-7. Ini dilakukan dengan menjalankan ujian sitotoksisiti dan menganalisis induksi apoptosis dan taburan kitaran sel menggunakan sitometri aliran. Kajian menunjukkan bahawa selepas 48 jam rawatan, nilai kepekatan perencatan separuh maksimum (IC_{50}) untuk RL-AgNPs didapati masing-masing adalah 67.42 dan 7.4 µg/mL dalam sel HepG2 dan MCF-7. Sitometri aliran mendedahkan peningkatan ketara dalam sel apoptosis dan nekrotik dalam kumpulan yang dirawat RL-AgNPs berbanding kumpulan kawalan dalam kedua-dua keluaran sel dan perubahan dalam sebahagian sel yang dikekalkan dalam fasa kitaran sel yang berbeza berbanding dengan kumpulan kawalan. Tambahan pula, didapati bahawa RL-AgNPs (IC_{50}) menyebabkan apoptosis dalam HepG2 dan MCF-7, seperti yang ditunjukkan oleh pengumpulan fasa sub-G1. Kesimpulannya, RL-AgNPs mempunyai potensi sebagai agen antikanser yang boleh dipercayai disebabkan keupayaan untuk mendorong apoptosis sel kanser, dengan itu memudahkan keluaran dari kitaran sel. Keupayaan ini boleh memberi kesan ketara kepada perkembangan ubat terapeutik untuk rawatan kanser masa hadapan.

Kata kunci: Nanopartikel perak, ramnolipid, HepG2, MCF-7, sitotoksisiti

Introduction

Cancer is a significant disease, causing high mortality rates in both developing and developed nations. In 2012, there were 14.1 million documented instances of cancer globally. The incidence of cancer is projected to rise by around 70% by the year 2035 [1]. Liver cancer ranks as the third biggest cause of mortality among various cancer types, while breast cancer remains a prevalent form of cancer among women worldwide [2, 3]. Nanotechnology has attracted significant attention owing to its prospective uses in the biomedical field, particularly in the creation of agents with diverse properties [4]. Metal nanoparticles (MNPs) exhibit unique magnetic and optical properties, a high surface area-to-volume ratio, low melting points, and exceptional mechanical strength. These characteristics make them appropriate for use in both medical and industrial sectors [5]. Furthermore, these attributes provide advantages in diagnostics, medication administration, and bio-imaging [6].

Silver nanoparticles (AgNPs) have attracted considerable interest among metallic nanoparticles (MNPs) owing to their distinctive biological and physicochemical characteristics [7]. Silver nanoparticles (AgNP) may be synthesised using several processes, including chemical precipitation, reverse micelle technique, chemical vapour deposition, hydrothermal method, microwave synthesis, and biological approaches [8-13]. Nonetheless, physicochemical techniques for nanoparticle synthesis include several disadvantages, including the use of hazardous surfactants, the generation of toxic by-products, the need for non-standard reaction conditions, and challenges associated with particle aggregation. There is now considerable emphasis on the ecologically sustainable manufacture, or green synthesis, of nanoparticles using biosurfactants and biological components, owing to the amalgamation of hazardous and toxic compounds with chemical processes [14-16].

Recent years have seen many study on AgNPs owing to their potential as bioactive agents against several pathogenic bacteria and cancer cell lines [17-19]. Numerous studies have shown that AgNPs have a significant capacity to trigger apoptosis or necrosis in various cell types [20-23]. A recent study investigating the cytotoxic and genotoxic effects of AgNPs on human cells has shown that AgNPs can disrupt mitochondrial function, stimulate the generation of reactive oxygen species (ROS), induce chromosomal abnormalities, and ultimately inflict DNA damage. Cell cycle arrest transpires after these effects [24, 25].

This study aims to investigate the cytotoxicity, apoptosis, and necrosis effects of rhamnolipid-synthesised AgNPs on *in vitro* cultures of human hepatocellular (HepG2) and breast (MCF-7) cancer cells. The sulforhodamine B (SRB) assay was used to analyse the growth inhibition of both cell lines. Additionally, cellular morphology was examined. Furthermore, an investigation was conducted to assess the possible impact of AgNPs on the apoptosis and disruption of the cell cycle. The findings obtained from this study have the potential to provide a novel strategy for effective chemotherapy treatment in individuals diagnosed with cancer.

Materials and Methods

Preparation of cell culture

Hepatocellular carcinoma (HepG2) and breast adenocarcinoma (MCF-7) were obtained from the American Tissue Culture Collection (ATCC). The cells were propagated in Dulbecco's modified eagle medium (DMEM) media containing 100 mg/mL of streptomycin, 100 units/mL of penicillin and 10% of heat-inactivated foetal bovine serum (FBS). The cultures were maintained in a humidified environment with 5% (v/v) CO_2 at a temperature of 37°C.

Preparation of silver nanoparticles (AgNPs)

Prior AgNP biosynthesis, RL was first constructed according to Azemi et al. [26]. The fermentation of RL from *P. aeruginosa* UMTKB-5 (GenBank accession no. KT194193.1), a marine sediment isolate, was first carried out in mineral salt medium (MSM) supplemented by trace elements solution (TE) and 20 g/L of glycerol as a carbon source at 30°C and 200 rpm for 72 h, followed by centrifugation and extraction using the acid precipitation method.

Subsequently, AgNP biosynthesis was carried out as described by Atwan and Hayder with modifications [27]. The RL in Milli-Q water (100 mg/L) (dispersed for 20 min by sonication) was mixed with $AgNO_3$ in Milli-Q water (0.006 M). The pH was maintained at 9 using 0.1 N NaOH and 0.1 N HCl, followed by an incubation for 72 h. The AgNPs were centrifuged and rinsed thrice with Milli-Q water. The solution containing AgNPs was placed in the freezer overnight at -80°C until transferred to a Freezer Dry System (Labconco, US) for 48 h before being used for subsequent analyses.

Cytotoxicity of AgNPs by sulforhodamine B (SRB) assay

The cytotoxicity of the RL-AgNPs was tested against HepG2 cells and MCF-7 cells by SRB assay. Briefly, aliquots of 100 µL of cell suspension ($5x10^3$ cells) were seeded in 96-well plates and incubated in complete media for 24 h. Cells were exposed to RL-AgNPs for 72 hours at several different concentrations: for MCF-7 (1, 3, 10, 30, 100 µg/mL) and for HepG2 (10, 25, 50, 100, 200 µg/mL). The cells were then fixed by replacing media with 150 µL of 10% trichloroacetic acid TCA and incubating for 1 h at 4°C. The cells were washed five times with distilled water after removing the TCA solution. Then 70 µL of SRB solution (0.4% w/v) was added and incubated in a dark place at room temperature for 10 min and washed thrice with 1% acetic acid before being left to air-dry overnight. 150 µL of TRIS solution (10 mM, pH 10.5) was used to dissolve the protein-bound SRB stain, and the absorbance was measured at 540 nm using a BMG LABTECH®- FLUOstar Omega microplate reader (Ortenberg, Germany) [28]. An assay was performed using three replicates for each cell line, and an average was calculated for each set. The IC_{50}, or inhibitory concentration of RL-AgNPs, was used to measure the cytotoxicity of nanoparticles, which is the concentration of nanoparticles that reduces cell survival by 50% compared to the control. Finally, 50% inhibitory concentration (IC_{50}) was calculated using the GraphPad Prism 9.0 software. The cell viability was determined by the following equation, where OD refers to optical density:

$$Cell\ viability\ (\%) = \frac{(Mean\ OD\ value\ of\ AgNPs-treated\ cells}{Mean\ OD\ value\ of\ untreated\ cells\ or\ control} x\ 100 \quad (1)$$

Morphology examination and apoptosis detection

After treating HepG2 cells with RL-AgNPs at concentrations of 10, 50, and 200 µg/mL, and MCF-7 cells at concentrations of 10, 30, and 100 µg/mL for 72 h, cell morphological changes were examined by an inverted microscope (TCM 400, LABOMED, US). Untreated cells were also included. The apoptosis and necrosis in HepG2 and MCF-7 cells were determined using the Annexin V-FITC apoptosis detection kit (Abcam, UK) coupled with two fluorescent channels flow cytometry. For this task, HepG2 and MCF-7 (10^5 cells) were cultured in 96-well microplates. After 48 h of treatment with the IC_{50} concentration of AgNPs, control and treated cells were treated with trypsin and washed twice with ice-cold PBS (pH 7.4). The cells were then incubated in the dark for 30 min with 0.5 mL of Annexin V-FITC/PI solution at room temperature, according to the manufacturer's instructions. Following

staining, cells were placed in ACEA Novocyte flow cytometer instrument (ACEA Biosciences, US) to analyse the fluorescent signals of FITC and PI using FL1 and FL2 signal detectors, respectively. ($\lambda_{ex/em}$ 488/530 nm for FITC and $\lambda_{ex/em}$ 535/617 nm for PI). A total of 12,000 events were collected for each sample, and the number of positive FITC and/or PI cells was determined through quadrant analysis and computed using ACEA NovoExpress software (ACEA Biosciences, US) [29]. The experiment was performed in triplicates, and the result was represented as mean ± standard deviation.

Cell cycle analysis by flow cytometry

Cells (10^5 cells) were plated in 96-well microplates to evaluate the impact of RL-AgNPs on cell cycle distribution. After treatment with IC_{50} concentration of RL-AgNPs for 48 h, cells were treated with trypsin and washed twice with ice-cold PBS (pH 7.4). Total 2 mL of 60% ice-cold ethanol were slowly added while shaking, and cells were kept at 4ºC for 1 h for fixation. Fixed cells were washed twice again with PBS (pH 7.4) and re-suspended in 1 mL of PBS containing 50 µg/mL RNase A and 10 µg/mL propidium iodide (PI). After 20 min of incubation in the dark at 37°C, cells were analysed for DNA contents using flow cytometry analysis equipped with FL2 ($\lambda_{ex/em}$ 535/617 nm) signal detector (ACEA Novocyte flowcytometer, ACEA Biosciences, US). A total of 12,000 events were collected per sample. ACEA NovoExpress software was used to compute the cell cycle distribution [30].

Statistical analysis

Statistical analysis was conducted using One-Way Analysis of Variance (ANOVA), followed by Tukey's multiple comparisons test, employing GraphPad Prism 9.0 software (GraphPad Software, US). This software was utilised for all statistical analyses to assess the significance of the studied data. A 95% confidence level (p <0.05) was considered statistically significant, and data were presented as the mean ± standard deviation.

Results and Discussion

Cell viability analysis

The effects of RL-AgNPs were investigated on two distinct cancer cell lines (HepG2 and MCF-7) using SRB assay. The binding of the SRB dye with cellular amino acids/proteins is responsible for its colorimetric estimation, which allows for measuring the total protein content within the identified cell. The results revealed that treatment with RL-AgNPs sharply reduced the viability of the HepG2 and MCF-7 cancer cell lines in a concentration-dependent manner (Figure 1). For the MCF-7 cell line, the viability for the highest concentration of RL-AgNPs (100 µg/mL) was approximately 0.73 ± 0.14%, while the HepG2 cancer cell line had 3.77 ± 0.01% viability for the same concentration. RL-AgNPs at the concentration of 10 µg/mL did not significantly reduce HepG2 cell viability. In contrast, the minimum concentration of RL-AgNPs that cause cytotoxicity in MCF-7 cells was 3 µg/mL. These results suggested that the human liver is more resistant to RL-AgNPs exposure as compared to breasts. The IC_{50} value indicates the concentration at which a 50% inhibitory effect is observed, indicating cytotoxicity. The RL-AgNPs exhibited the more potent cytotoxicity response against MCF-7 cell lines, as evidenced by an IC_{50} of 7.4 ± 0.6 µg/mL. On the other hand, the efficacy of RL-AgNPs against cancer HepG2 cell lines was less potent, with an IC_{50} of 67.42 ± 0.6 µg/mL.

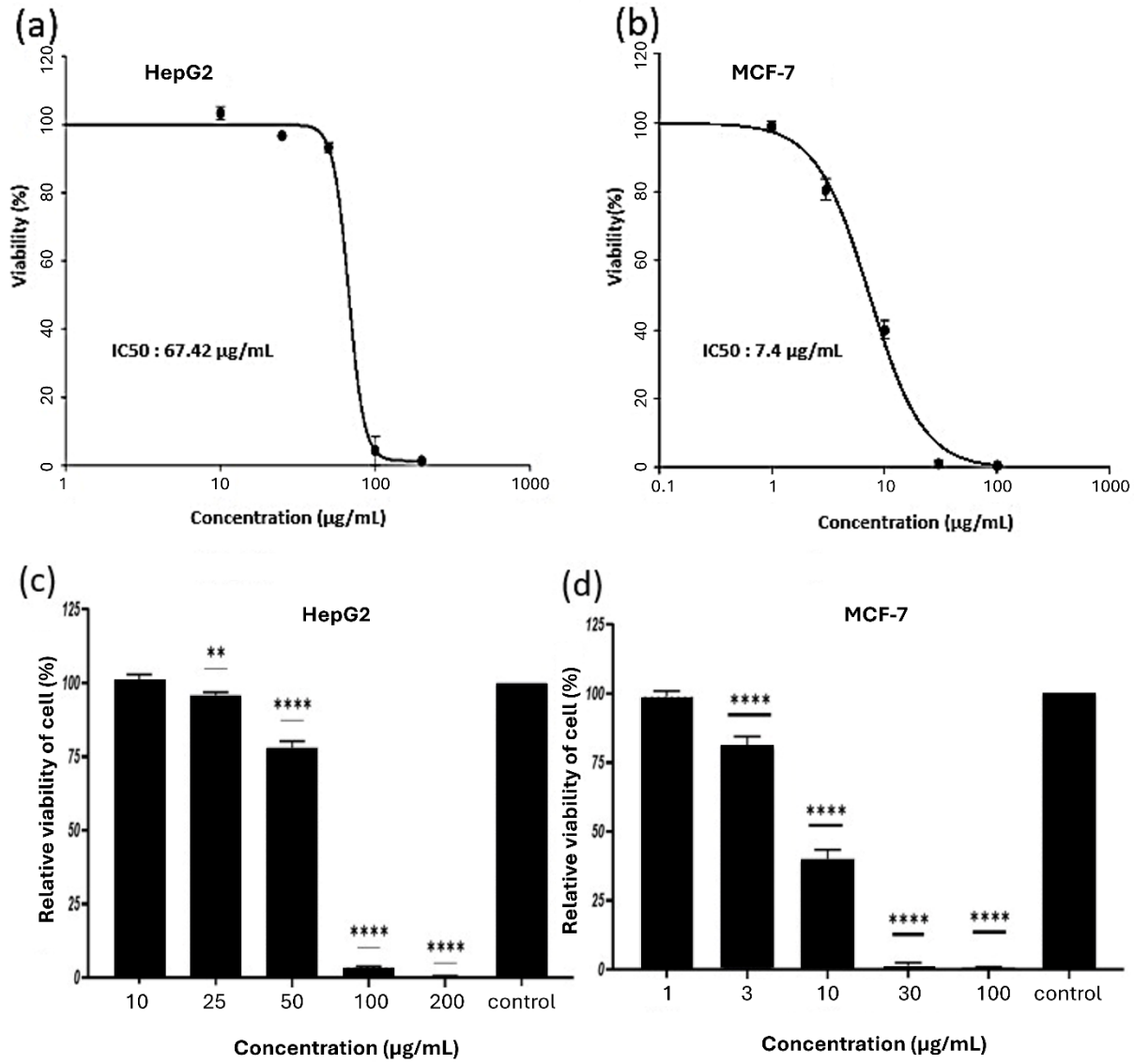

Figure 1. Graphs from cell viability analysis. Dose-response inhibitory curve and growth inhibitory concentration (IC_{50}) values after 72 h of RL-AgNPs in (a) HepG2 and (b) MCF-7 cancer cell lines. The relative viability percentage and anti-proliferative effect of RL-AgNPs with respect to (c) HepG2 and (d) MCF-7. One-way ANOVA is performed, followed by Tukey's multiple comparisons test for analysis. Results are expressed as mean ± SD (** $p \leqslant 0.01$; **** $p \leqslant 0.0001$) compared with control

Morphology examination

The morphologies of HepG2 and MCF-7 were examined using an inverted microscope after treatment with RL-AgNPs. The micrographs indicated that treatment with RL-AgNPs resulted in significant morphological changes and apoptotic features in both cancer cell lines, including irregular distribution, cytoplasmic contraction, and cellular rounding (Figure 2). Two different ranges of RL-AgNP concentrations were tested on HepG2 and MCF-7 cell lines to investigate the effect of RL-AgNPs on each cell line separately and to adjust with the higher sensitivity of MCF-7 towards RL-AgNPs. In-depth comparative research of different cell lines across a standardised range of concentration could uncover future insightful comprehension of the RL-AgNPs studied. A reduction in cell population was seen

when the concentration of AgNPs escalated. The RL-AgNPs-treated MCF-7 cell line demonstrated significant growth inhibition, resulting in almost complete cell death at doses of 30 µg/mL and higher concentrations. This cell line exhibited heightened sensitivity to RL-AgNPs, resulting in a significant reduction in cell count. This outcome corroborated our results about the previously reported IC_{50} and cell viability metrics. Conversely, cells in the untreated groups seemed normal regarding shape and quantity. These results further substantiate the importance of AgNPs in cancer treatment and their cytotoxic effects on HepG2 and MCF-7 cells [31, 32].

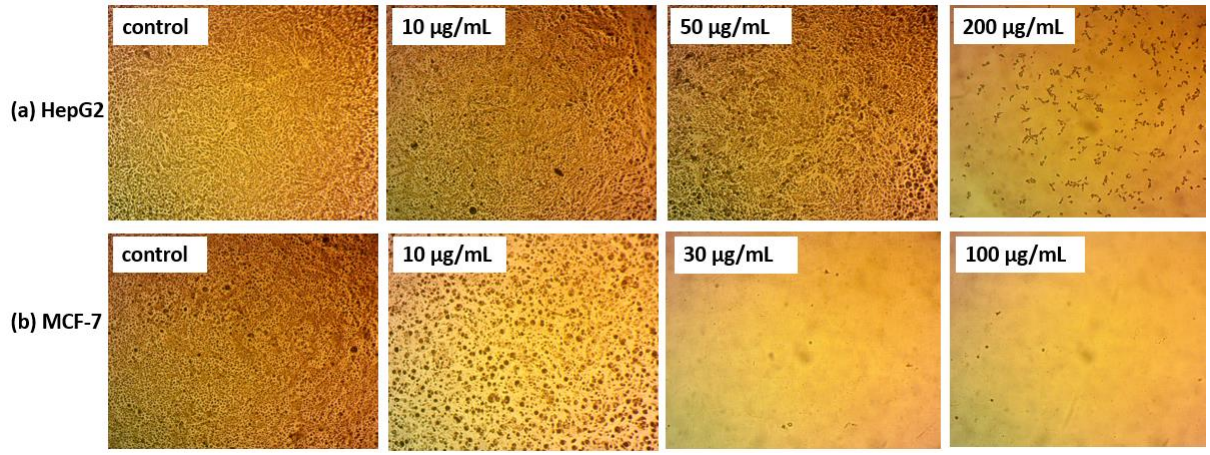

Figure 2. Micrographs from morphological analysis using inverted microscope (100X) of (a) HepG2 (b)MCF-7 treated with RL-AgNPs at different concentrations (HepG2 cells with RL-AgNPs at concentrations of 10, 50, and 200 µg/mL, and MCF-7 cells at concentrations of 10, 30, and 100 µg/mL for 72 h) and untreated cells (negative control)

Effects of RL-AgNPs on cell apoptosis

The Annexin V-FITC apoptosis assay was used to differentiate between apoptotic and necrotic cell populations. It is based on the binding capabilities of Annexin V for phosphatidylserine (PS), a lipid generally found on the cell membrane's inner leaflet. PS becomes externalised on the outside leaflet of the cell membrane during apoptosis, making it accessible to Annexin V. This enables Annexin V to attach precisely to apoptotic cells [33]. Moreover, propidium iodide (PI) dye binds to the fragmented DNA of dead cells [34]. Flowcytometer device enables the differentiation of the stained cells into four distinct groups: viable (annexin V- PI-), cells in the early stages of apoptosis (annexin V+ PI-), cells in the late stages of apoptosis (annexin V+ PI+), and cells undergoing necrosis (annexin V- PI+). After HepG2 cells and MCF-7cells were treated with IC_{50} of RL-AgNPs for 48 h, cells were stained with Annexin V-FITC and PI, which can distinguish between viable, early apoptotic, late apoptotic, and necrotic cell populations (Figure 3).

When comparing to the control group (untreated cells), we found that treatment with RL-AgNPs at IC_{50} concentration dramatically decreased the number of viable HepG2 cells to 91.63 ± 0.33% (p <0.0001) and significantly increased the percentage of necrotic and late apoptosis cells to 6.68 ± 0.22% and 1.68±0.11%, respectively. On the other hand, MCF-7 cells displayed a more dramatic response to RL-AgNPs treatment at the IC_{50} concentration. The MCF-7 viable cell was dramatically reduced to 80.50 ± 0.62% after treatment with RL-AgNPs at the IC_{50} level, while late apoptotic cells were significantly increased to 17.57 ±0.50% (p <0.0001). Conversely, like HepG2, no significant differences were observed in the early apoptosis stage. Remarkable reduction in viable cells occurred for both cell lines, indicating the potential use of the synthesized RL-AgNPs in cancer therapy by activating apoptotic and necrotic pathways. Previous studies on the effects of

green-synthesised AgNPs against cancer cell lines were chiefly derived from plant extracts, such as *Indigofera heterantha*, *Ocimum americanum*, and *Dicoma anomala* [35-37]. A recent study by El-Deeb et al. investigated cyanobacterial *Arthrospira platensis*-mediated green biosynthesis of silver nanoparticles that displayed dose-dependent cytotoxic effects against HepG-2 and MCF-7 cell lines as well as apoptosis, which was in line with the findings of the present study [38].

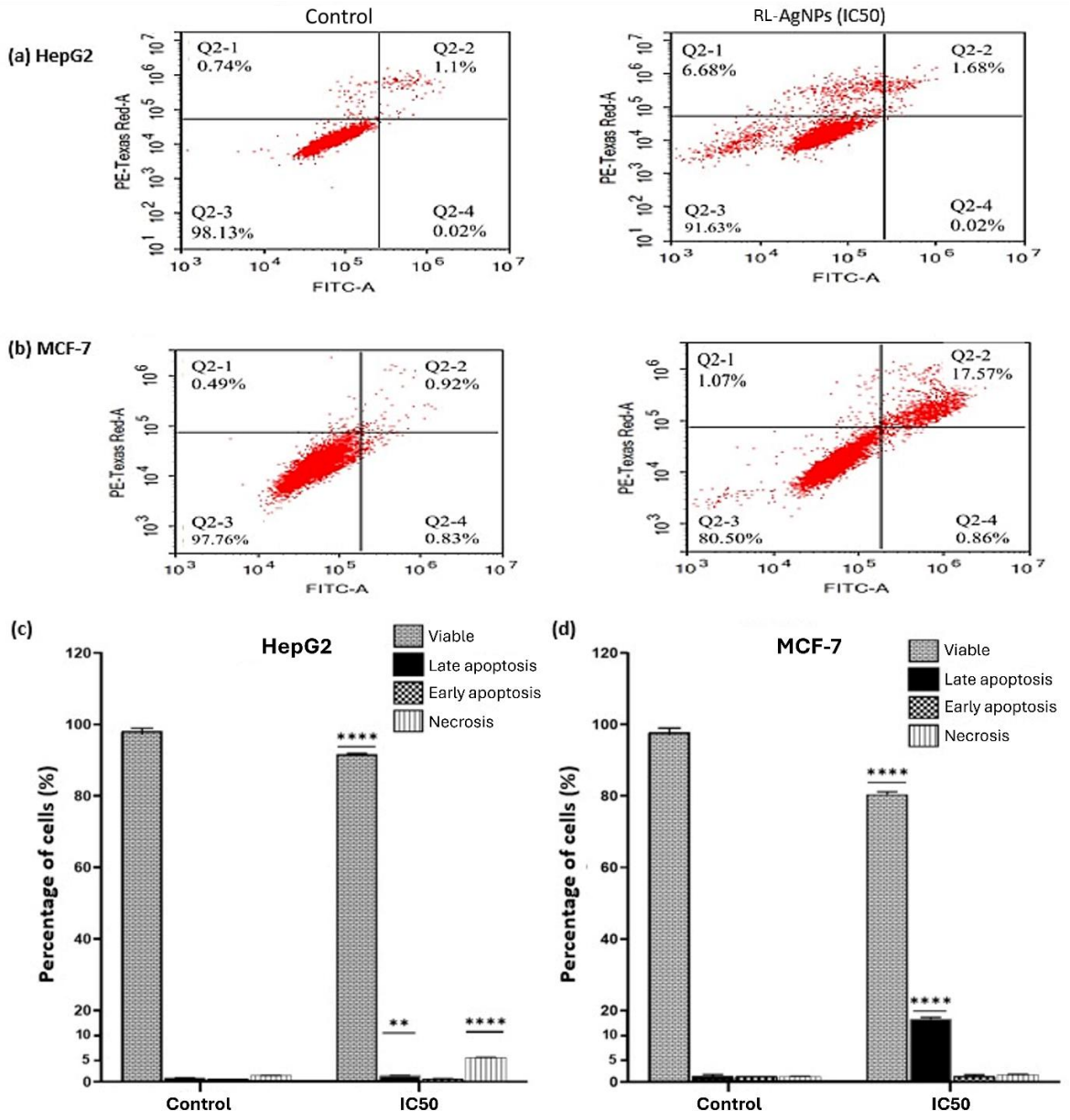

Figure 3. Apoptosis using flow cytometry induced by RL-AgNPs after 48 h in (a) HepG2 and (b) MCF7 cells. The flow cytometry graph's four quadrants represent necrotic (Q1), Late apoptotic (Q2), viable(Q3), and early apoptotic (Q4) cells. The Bar chart shows the percentage of early apoptotic cells, late apoptotic cells and necrotic cells with respect to negative control (untreated) for (c) HepG2 and MCF-7. Results are expressed as mean ± SD (** $p \leqslant 0.01$; **** $p \leqslant 0.0001$) compared with control

Effects of RL-AgNPs on Cell Cycle

After treatment with RL-AgNPs at IC_{50} concentrations for 48 h, HepG2 and MCF-7 cells were collected, fixed, and stained with propidium iodide in succession. A flow cytometer was used to evaluate the cell populations in each phase. A sub-population appeared prior to the G1 peak in cells subjected to cytotoxic or apoptosis-inducing chemicals, referred to as the sub-G1 (apoptosis) peak. This population exhibiting reduced stability is believed to arise from endonuclease activation, resulting in DNA leaking from the cells. The contrast between apoptotic and necrotic cells are evident, since necrotic cells do not demonstrate a rapid decline in DNA content [39, 40]. Treatment of HepG2 cells with IC_{50} concentration of RL-AgNPs increased the percentage of cells in the sub-G1 phase to 9.17± 0.46 %, compared to 1.03 ± 0.11% in control cells (p<0.0001). However, in the G2 phase, there was a decrease in the percentage of cells to 18.50± 0.33% compared to 24.56 ±3.21% in the control cells (p<0.001). There were no significant differences in the G1 and S phases compared to control (Figure 4).

In the case of MCF-7, Treatment with RL-AgNPs for 48 h highly increased sub-G1 cells to 28.61± 0.50 compared to 1.09 ±0.11% in control cells and significantly decreased G1 phase cells to 33.75±0.58 compared to 67.17±2.55% in control cells (p<0.0001). The cell cycle consists of interphases (G1, S, and G2) and mitosis (M). During the G1 phase, cells experience cellular growth, RNA synthesis, and protein manufacturing to support DNA replication. DNA replication transpires during the S phase of the cell cycle, as cells persist in their expansion. During the G2 phase, additional proteins are synthesised as the cell progresses to the M phase, characterised by cytoplasmic and nuclear divisions [41]. A fundamental strategy in the development of anticancer pharmaceuticals is the regulation of the cancer cell cycle [42-44].

Conclusion

The study demonstrated cytotoxicity, necrosis, and late apoptosis of RL-AgNPs in HepG2 and MCF-7 cancer cell lines. The effectiveness of RL-AgNPs is dose-dependent and varies in terms of susceptibility. The RL-AgNPs showed the highest potency against MCF-7 cells. The findings further indicated that RL-AgNPs at the IC_{50} concentration induced late apoptosis and cell cycle arrest. This is the first report on the cytotoxicity and late apoptosis of AgNPs synthesised using a marine bacterium-derived rhamnolipid from the isolate, *P. aeruginosa* UMTKB-5, against HepG2 and MCF-7 cells. Further research and *in vivo* analyses of the green-synthesised AgNPs could investigate its potential for cancer treatment.

Acknowledgement

This study was partially supported by Postgraduate Research Grant (PGRG), Research Management and Innovation Centre (RMIC), Universiti Malaysia Terengganu (UMT), grant number 55193/1.

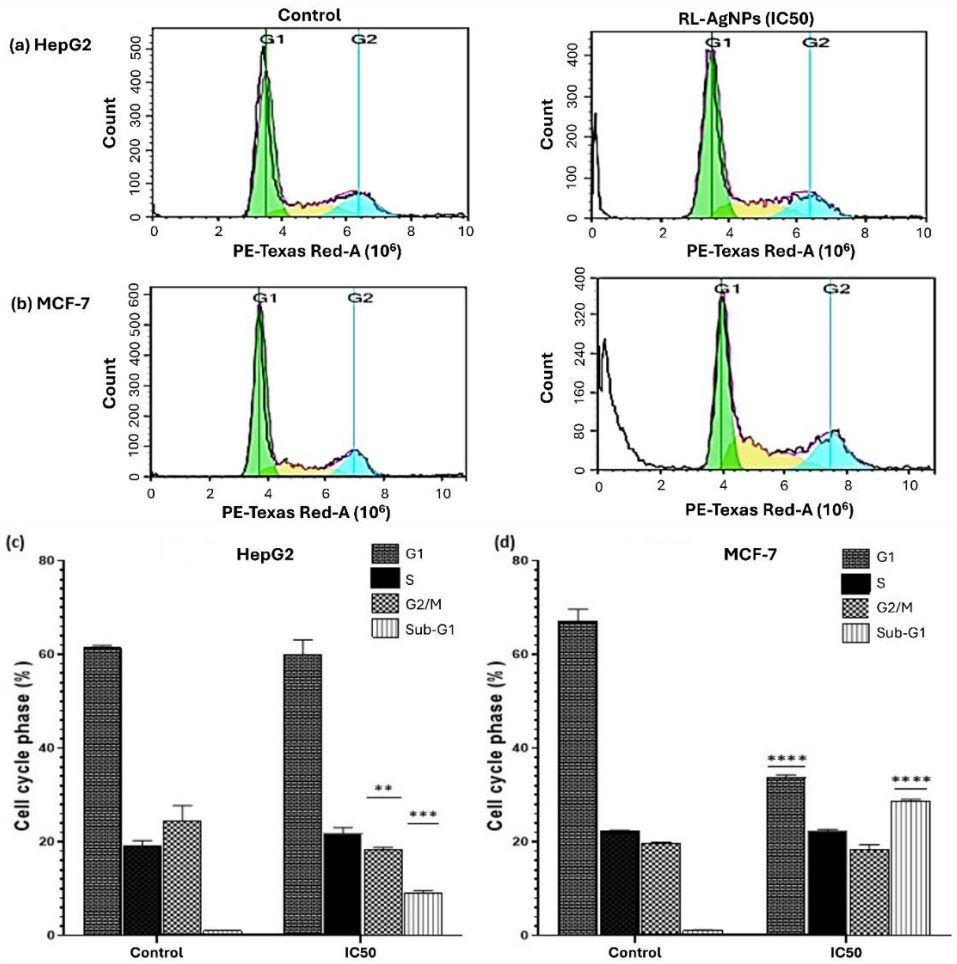

Figure 4. Cell cycle analysis of (a) HepG2 cells and (b) MCF-7 cells treated with IC50 of RL-AgNPs for 48 h. (c)The Bar chart represents the quantitative results of various cell cycle phases, including G1, S, and G2/M. SubG1 reflects the percentage of cells that have undergone apoptosis. Results are expressed as mean ± SD (** $p \leqslant 0.01$; *** $p \leqslant 0.001$; **** $p \leqslant 0.0001$) compared with control

References

1. Vainshelboim, B., Müller, J., Lima, R. M., Nead, K. T., Chester, C., Chan, K., Kokkinos, P., and Myers, J. (2017). Cardiorespiratory fitness and cancer incidence in men. *Annal Epidemiology*, 27(7): 442-447.
2. Huang, D. Q., Singal, A. G., Kono, Y., Tan, D. J. H., El-Serag, H. B., and Loomba, R. (2022). Changing global epidemiology of liver cancer from 2010 to 2019: NASH is the fastest growing cause of liver cancer. *Cell Metabolism*, 34(7): 969-977.
3. Orlandella, F. M., De Stefano, A. E., Iervolino, P. L. C., Buono, P., Soricelli, A., and Salvatore, G. (2021). Dissecting the molecular pathways involved in the effects of physical activity on breast cancers cells: A narrative review. *Life Sciences*, 265: 118790.
4. Abd Elkodous, M., El-Sayyad, G. S., Abdelrahman, I. Y., El-Bastawisy, H. S., Mohamed, A. E., Mosallam, F. M., Nasser, H. A., Gobara, M., Baraka, A., Elsayed, M. A., and El-Batal, A. I. (2019). Therapeutic and diagnostic potential of nanomaterials for enhanced

biomedical applications. *Colloids Surface B Biointerfaces*, 180: 411-428.

5. Wahab, R., Siddiqui, M. A., Saquib, Q., Dwivedi, S., Ahmad, J., Musarrat, J., Al-Khedhairy, A. A., and Shin, H. S. (2014). ZnO nanoparticles induced oxidative stress and apoptosis in HepG2 and MCF-7 cancer cells and their antibacterial activity. *Colloids Surface B Biointerfaces*, 117: 267-276.
6. Thirumalai, J. (2023). *Quantum Dots - Recent Advances, New Perspectives and Contemporary Applications*. IntechOpen, Austria: pp. 264.
7. Zhang, J., Guo, W., Li, Q., Wang, Z., and Liu, S. (2018). The effects and the potential mechanism of environmental transformation of metal nanoparticles on their toxicity in organisms. *Environmental Sciences: Nano*, 5(11): 2482-2499.
8. Beier, O., Pfuch, A., Horn, K., Weisser, J., Schnabelrauch, M., and Schimanski, A. (2012). Low temperature deposition of antibacterially active silicon oxide layers containing silver nanoparticles, prepared by atmospheric pressure plasma chemical vapor deposition. *Plasma Process Polymers*, 10(1): 77-87.
9. Hong, X., Wen, J., Xiong, X., and Hu, Y. (2016). Shape effect on the antibacterial activity of silver nanoparticles synthesized via a microwave-assisted method. *Environmental Science Pollution Research International*, 23(5): 4489-4497.
10. Lengke, M. F., Fleet, M. E., and Southam, G. (2007). Biosynthesis of silver nanoparticles by filamentous cyanobacteria from a silver(I) nitrate complex. *Langmuir*, 23(5): 2694-2699.
11. Lu, W., Liao, F., Luo, Y., Chang, G., and Sun, X. (2011). Hydrothermal synthesis of well-stable silver nanoparticles and their application for enzymeless hydrogen peroxide detection. *Electrochimica Acta*, 56(5): 2295-2298.
12. Narayanan, M., Divya, S., Natarajan, D., Senthil-Nathan, S., Kandasamy, S., Chinnathambi, A., Alahmadi, T. A., and Pugazhendhi, A. (2021). Green synthesis of silver nanoparticles from aqueous extract of *Ctenolepis garcini* l. and assess their possible biological applications. *Process Biochemistry*, 107: 91-99.
13. Singha, D., Barman, N., and Sahu, K. (2014). A facile synthesis of high optical quality silver nanoparticles by ascorbic acid reduction in reverse micelles at room temperature. *Journal of Colloid Interface Sciences*, 413: 37-42.
14. Das, M., Borah, D., Patowary, K., Borah, M., Khataniar, A., and Kakoti, B.B. (2019). Antimicrobial activity of silver nanoparticles synthesised by using microbial biosurfactant produced by a newly isolated *Bacillus vallismortis* MDU6 strain. *IET Nanobiotechnology*, 13(9): 967-973.
15. Kasture, M., Patel, P., Prabhune, A., Ramana, C. V., Kulkarni, A. A., & Prasad, B. L. V. (2008). Synthesis of silver nanoparticles by sophorolipids: Effect of temperature and sophorolipid structure on the size of particles. *Journal of Chemical Sciences*, 120(6): 515-520.
16. Kumar, C. G., Mamidyala, S. K., Das, B., Sridhar, B., Devi, G. S., and Karuna, M. S. (2010). Synthesis of biosurfactant-based silver nanoparticles with purified rhamnolipids isolated from *Pseudomonas aeruginosa* BS-161R. *Journal of Microbiology Biotechnology*, 20(7): 1061-1068.
17. Avalos, A., Haza, A. I., Mateo, D., and Morales, P. (2014). Cytotoxicity and ROS production of manufactured silver nanoparticles of different sizes in hepatoma and leukemia cells. *Journal Applied Toxicology*, 34(4): 413-423.
18. Kirmanidou, Y., Sidira, M., Bakopoulou, A., Tsouknidas, A., Prymak, O., Papi, R., Choli-Papadopoulou, T., Epple, M., Michailidis, N., Koidis, P., and Michalakis, K. (2019). Assessment of cytotoxicity and antibacterial effects of silver nanoparticle-doped titanium alloy surfaces. *Dental Materials*, 35(9): e220-e233.
19. Radzig, M. A., Nadtochenko, V. A., Koksharova, O. A., Kiwi, J., Lipasova, V. A., and Khmel, I. A. (2013). Antibacterial effects of silver nanoparticles on gram-negative bacteria: Influence on the growth and biofilms formation, mechanisms of action. *Colloids Surface B Biointerfaces*, 102: 300-306.
20. Barbasz, A., Oćwieja, M., and Roman, M. (2017). Toxicity of silver nanoparticles towards tumoral human cell lines U-937 and HL-60. *Colloids Surface B Biointerfaces*, 156: 397-404.
21. Foldbjerg, R., Dang, D. A., and Autrup, H. (2011). Cytotoxicity and genotoxicity of silver

nanoparticles in the human lung cancer cell line, A549. *Archives Toxicology*, 85(7): 743-750.

22. Hekmat, A., Saboury, A. A., and Divsalar, A. (2012). The effects of silver nanoparticles and doxorubicin combination on DNA structure and its antiproliferative effect against T47D and MCF7 cell lines. *Journal Biomedicine Nanotechnology*, 8(6): 968-982.
23. Juarez-Moreno, K., Gonzalez, E. B., Girón-Vazquez, N., Chávez-Santoscoy, R. A., Mota-Morales, J. D., Perez-Mozqueda, L. L., Garcia-Garcia, M. R., Pestryakov, A., and Bogdanchikova, N. (2017). Comparison of cytotoxicity and genotoxicity effects of silver nanoparticles on human cervix and breast cancer cell lines. *Human Exposure Toxicology*, 36(9): 931-948.
24. Gurunathan, S., Qasim, M., Park, C., Yoo, H., Kim, J. H., and Hong, K. (2018). Cytotoxic potential and molecular pathway analysis of silver nanoparticles in human colon cancer cells HCT116. *International Journal Molecular Science*, 19(8): 2269.
25. Jeyaraj, M., Renganathan, A., Sathishkumar, G., Ganapathi, A., and Premkumar, K. (2015). Biogenic metal nanoformulations induce Bax/Bcl2 and caspase mediated mitochondrial dysfunction in human breast cancer cells (MCF 7). *RSC Advances*, 5(3): 2159-2166.
26. Azemi, M. A., Rashid, N. F., Saidin, J., Effendy, A. W., and Bhubalan, K. (2016). Application of sweetwater as potential carbon source for rhamnolipid production by marine *Pseudomonas aeruginosa* UMTKB-5. *International Journal Bioscience Biochemistry Bioinformatics*, 6:50-58.
27. Atwan, Q. S., and Hayder, N. H. (2020). Eco-friendly synthesis of silver nanoparticles by using green method: Improved interaction and application *in vitro* and *in vivo*. *Iraqi Journal Agriculture Sciences*, 51:2010-2016.
28. Skehan, P., Storeng, R., Scudiero, D., Monks, A., McMahon, J., Vistica, D., Warren, J. T., Bokesch, H., Kenney, S., and Boyd, M. R. (1990). New colorimetric cytotoxicity assay for anticancer-drug screening. *Journal National Cancer Institute*, 82(13): 1107-1112.
29. Fekry, M. I., Ezzat, S. M., Salama, M. M., Alshehri, O. Y., and Al-Abd, A. M. (2019). Bioactive glycoalkaloides isolated from *Solanum melongena* fruit peels with potential anticancer properties against hepatocellular carcinoma cells. *Science Report*, 9(1): 1746.
30. Bashmail, H. A., Alamoudi, A. A., Noorwali, A., Hegazy, G. A., AJabnoor, G., Choudhry, H., and Al-Abd, A. M. (2018). Thymoquinone synergizes gemcitabine anti-breast cancer activity via modulating its apoptotic and autophagic activities. *Science Report*, 8(1): 11674.
31. Dwivedi, S., Saquib, Q., Al-Khedhairy, A. A., Ahmad, J., Siddiqui, M. A., & Musarrat, J. (2015). Rhamnolipids functionalized AgNPs-induced oxidative stress and modulation of toxicity pathway genes in cultured MCF-7 cells. *Colloids Surface B Biointerfaces*, 132: 290-298.
32. Vijayakumar, M., Priya, K., Ilavenil, S., Janani, B., Vedarethinam, V., Ramesh, T., Arasu, M. V., Al-Dhabi, N. A., Kim, Y. O., and Kim, H. J. (2020). Shrimp shells extracted chitin in silver nanoparticle synthesis: Expanding its prophecy towards anticancer activity in human hepatocellular carcinoma HepG2 cells. *International Journal Biology Macromolecule*, 165(Pt A): 1402-1409.
33. Wani, M. Y., Ahmad, A., Aqlan, F. M., and Al-Bogami, A. S. (2020). Azole based acetohydrazide derivatives of cinnamaldehyde target and kill *Candida albicans* by causing cellular apoptosis. *ACS Medicine Chemistry Letters*, 11(4): 566-574.
34. Fard, S. E., Tafvizi, F., and Torbati, M. B. (2018). Silver nanoparticles biosynthesised using *Centella asiatica* leaf extract: Apoptosis induction in MCF-7 breast cancer cell line. *IET Nanobiotechnology*, 12(7): 994-1002.
35. Ullah, I., Khalil, A. T., Zia, A., Hassan, I., and Shinwari, Z. K. (2024). Insight into the molecular mechanism, cytotoxic, and anticancer activities of phyto‐reduced silver nanoparticles in mcf‐7 breast cancer cell lines. *Microscopy Research Technology*, 87(7): 1627-1639.
36. Alex, A. M., Subburaman, S., Chauhan, S., Ahuja, V., Abdi, G., and Tarighat, M. A. (2024). Green synthesis of silver nanoparticle prepared with ocimum species and assessment of anticancer potential. *Science Report*, 14(1): 11707.
37. Chota, A., Abrahamse, H., and George, B. P. (2024).

Green synthesis and characterization of AgNPs, liposomal loaded AgNPs and ZnPCs4 photosensitizer for enhanced photodynamic therapy effects in MCF-7 breast cancer cells. *Photodiagnosis Photodyn Therapy*, 48: 104252.

38. El-Deeb, N. M., Abo-Eleneen, M. A., Awad, O. A., and Abo-Shady, A. M. (2022). Arthrospira cytotoxicity, cell-cycle arrest, and apoptotic induction by *Euphorbia hirta* in MCF-7 breast cancer cells. *Pharmaceutical Biology*, 54(7): 1223-1236.
40. Namvar, F., Rahman, H. S., Mohamad, R., Baharara, J., Mahdavi, M., Amini, E., Chartrand, M. S., and Yeap, S. K. (2014). Cytotoxic effect of magnetic iron oxide nanoparticles synthesized via seaweed aqueous extract. *International Journal of Nanomedicine*, 9: 2479-2488.
41. Moghaddam, A. B., Moniri, M., Azizi, S., Abdul Rahim, R., Bin Ariff, A., Navaderi, M., and Mohamad, R. (2017). Eco-friendly formulated zinc oxide nanoparticles: Induction of cell cycle arrest and apoptosis in the MCF-7 cancer cell line. *Genes*, 8(10): 281.

platensis-mediated green biosynthesis of silver nano-particles as breast cancer controlling agent: *in vitro* and *in vivo* safety approaches. *Applied Biochemistry Biotechnology*, 194(5): 2183-2203.

39. Kwan, Y. P., Saito, T., Ibrahim, D., Al-Hassan, F. M., Ein Oon, C., Chen, Y., Jothy, S. L., Kanwar, J. R., and Sasidharan, S. (2016). Evaluation of the
42. Al-Majeed, S. H. A., Al-Ali, Z. S. A., and Turki, A. A. (2023). Biomedical assessment of silver nanoparticles derived from l-aspartic acid against breast cancer cell lines and bacteria strains. *BioNanoScience*, 13(4): 1833-1848.
43. Holmila, R. J., Vance, S. A., King, S. B., Tsang, A. W., Singh, R., and Furdui, C. M. (2019). Silver nanoparticles induce mitochondrial protein oxidation in lung cells impacting cell cycle and proliferation. *Antioxidants (Basel, Switzerland)*, 8(11): 552.
44. Sun, Y., Liu, Y., Ma, X., and Hu, H. (2021). The influence of cell cycle regulation on chemotherapy. *International Journal Molecule Sciences*, 22(13): 6923.